NASA TN D-1550

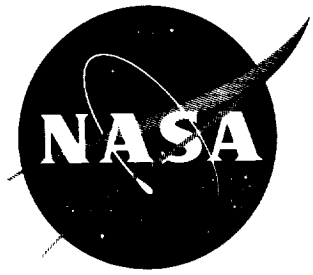

TECHNICAL NOTE

D-1550

HELIUM FILM COOLING ON A HEMISPHERE

AT A MACH NUMBER OF 10

By Robert E. Dannenberg

Ames Research Center
Moffett Field, Calif.

NATIONAL AERONAUTICS AND SPACE ADMINISTRATION

WASHINGTON

November 1962

NATIONAL AERONAUTICS AND SPACE ADMINISTRATION

TECHNICAL NOTE D-1550

HELIUM FILM COOLING ON A HEMISPHERE AT A MACH NUMBER OF 10

By Robert E. Dannenberg

SUMMARY

An experimental investigation has been made of the effectiveness of film cooling a hemisphere at a Mach number of 10 and a stagnation temperature of 8,700° R. Models tested were equipped for tangential injection at positions 5° and 10° downstream of the stagnation point. Helium was used as the coolant.

Measurements were made of the reduction in local heat transfer for various helium flow rates. The range of the ratio of the helium to air velocities at the air-helium interface at injection for these tests was from 1.2 to 6.

The results of the investigation indicate that film cooling was effective in reducing the heat transfer from the high-energy stream. The peak heating rate on a hemisphere was reduced by a factor of as much as 2.5 and immediately downstream of the injection port the surface was almost completely insulated from the air flow.

INTRODUCTION

Vehicles intended for travel at hypervelocities in the atmosphere must be provided with some type of thermal protection to maintain body temperatures at acceptable levels. For many applications, active cooling systems are being considered as a means of effective surface cooling, either as an alternative to, or in combination with, passive-type ablative or radiative systems. In an active system, material stored within a vehicle is supplied to the heated regions and in some way absorbs or blocks heat. One of the more promising methods is to inject a coolant gas into the gas layer adjacent to the surface. Two ways of injecting the gas are of interest: One is to inject a cool gas through a port or porous wall and allow it to mix with the hot air in the boundary layer. A second is to inject a cool gas tangentially from a slot so that it forms a separate insulating layer which does not mix with the hot air. This latter arrangement is designated as film cooling.

Ferri and Libby, in reference 1, discussed the idea of film cooling as applied to nozzles and showed that in an effective film-cooled system the molecular weight of the coolant gas is lower than that of the air. With such a coolant, the velocity of the high-temperature gas stream and of the coolant film can be essentially equal at the interface while the coolant temperatures are considerably less than those in the adjacent hot gas layer. Swenson's analysis in reference 2 shows the properties necessary for the injected gas to be an effective coolant; the molecular weight of the film gas should be low and its heat capacity should be high compared with air. Both references suggest that with properly matched air-coolant parameters at the injection slot, the coolant gas can flow tangentially back over the body with a minimum of mixing with the air, thus, providing a substantial reduction in heat transfer over an appreciable region of the body downstream of the stagnation region.

Experimental investigations to date on the effects of injecting a coolant gas from a port or a porous wall at the nose of a bluff body have been made in low-enthalpy flows (refs. 3 to 6). Generally, no strict accounting was taken of the air-coolant interface conditions.

The present tests were made to determine the effectiveness of film cooling in alleviating aerodynamic heating in a high enthalpy stream. Hemisphere models were equipped for tangential injection in the stagnation region. Helium was used as the coolant. Local heating rates over the hemisphere were determined under various conditions of coolant flow rate and ratios of helium-to-air velocities at the exit port. Comparison was then made with the analytical results of reference 2.

SYMBOLS

c_p specific heat of skin material, Btu/lb $^{\circ}F$

L thickness of skin material, ft

p local pressure on model, psf

q local heating rate, Btu/ft^2 sec

t time, sec

T temperature, $^{\circ}R$

V_a local value of air velocity at the cap exit location, fps

V_f local value of helium velocity at the cap exit, fps

w_f weight rate of film flow, lb/sec

θ angle between model axis and radial line on which a thermocouple is located, deg (see fig. 5)

ρ weight density of skin material, lb/cu ft

Subscripts

s stagnation

cal calculated

APPARATUS

Shock Tunnel

The heat-transfer tests reported herein have been made in the Ames 1-foot hypervelocity shock tunnel. The principle and operation of the tunnel is described in reference 7. Its basic components include:

1. Combustion driver section (oxygen-hydrogen combustion in a helium atmosphere)

2. Shock tube inlet section (diaphragm and throttling plates)

3. Shock tube section (6.2-inch dia. by 40-ft length)

4. Nozzle valve (programmed to close before driver gases enter nozzle)

5. Conical nozzle (9° expansion angle)

6. Test section (12-inch square)

7. Vacuum chamber

Some of the shock-tunnel details are illustrated in figure 1. Clean dry air was used as the driven, or test, gas. The duration of air flow in the test section is terminated by the closure of the nozzle valve. Test periods were from 80 to 150 milliseconds. A typical model installation is shown in figure 2. All the heating rates were obtained with the following nominal stream properties (see ref. 7):

Reynolds number per foot	58,700
Mach number	10
Total enthalpy of stream	4,510 Btu/lb
Stagnation temperature	8,700° R
Free-stream velocity	14,600 ft/sec
Pitot pressure	470 psf

A still camera was used to take luminosity photographs of each model tested. The intense illumination produced by the air in the shock layer also made it possible to take 16-mm motion pictures in color (500 frames/sec) during each run. This visual flow time-history was helpful as a monitoring device and also in providing qualitative information of the flow field.

Models

The models used in this investigation were 3-inch-diameter hemispheres. A plain model is shown in figure 3(a), and a model equipped for film injection is shown in figure 3(b). Details of the film-cooled models which illustrate the internal arrangement of the coolant passage and instrumentation are given in figure 4. The models were fabricated with wall thicknesses of about 0.020 to 0.030 inch by a technique combining thermo-forming and investment casting. Silicon bronze was used as the casting metal. Details of the manufacturing process are given in reference 8. The surface of the model as cast was sufficiently smooth that only polishing was required to provide an aerodynamically smooth surface. Number 36 gage (0.005-in. dia.) iron-constantan thermocouple wires were spot-welded to the interior surface of the skin. The two wires in each thermocouple were attached separately, immediately adjacent to one another but not touching. The helium gas used in the film-cooling tests was fed from a high-pressure source through the junction box and sting support to a sonic orifice located within the model. The sonic orifice consisted of one to four 0.035-inch-diameter holes. From the orifice, the gas exhausted into the plenum chamber behind the nose cap. The pressure in the plenum chamber was regulated, for a given orifice size, by adjusting the gap between the nose cap and the model skin. The gap settings for the largest coolant flow rates tested were about 0.011 inch.

TEST PROCEDURE

The helium mass flow through the models equipped for film cooling was regulated by the sonic orifices and the supply pressure. The injection velocity at the cap exit was regulated by the pressure in the plenum chamber. It was assumed that the addition of the contoured cap

would not change the magnitude and distribution of the local external pressures over the hemisphere as compared to the plain model. Pressures over the body were calculated from the stagnation pressure in the test section and the assumption of a modified Newtonian pressure distribution. Before a test run, each model was calibrated as follows: The pressure in the test section was reduced to a value that calculations indicated would exist at the cap exit during the actual test (about 470 psfa). Helium flow was initiated and the supply-line pressure ratio across the orifices was kept sufficiently large to insure sonic flow in the orifices. The pressure value in the plenum chamber and the calculated body pressure at the cap exit were then used to determine the film velocity (subsonic) from the isentropic flow relations. To adjust the film velocity, it was necessary to reset the gap or change the number of orifices in the model. Once the necessary settings were established, the model was ready to test.

Before each test run the test section was evacuated to less than 125 microns of mercury. Onset of helium flow was controlled by a solenoid valve programmed to open just before the air flow started in the test section.

The weight rate of the film flow, w_f, for each test was measured to an accuracy within ±3 percent; however, the corresponding ratio of the film velocity to the local surface velocity at the body station of the cap exit was not as closely determined. The temperature of the helium was assumed to remain at that of the plenum chamber until after it passed the gap exit. The local air velocity, V_a, at the cap exit station was determined from the Newtonian impact pressure at that body station, entropy based on stagnation conditions, and the Mollier diagram. The over-all accuracy of the ratio V_f/V_a was estimated to be better than ±25 percent.

DATA REDUCTION

Test data were secured in the form of analog signals produced by the iron-constantan thermocouples in the model and by the pressure transducer for the coolant system. The transient output signals from the thermocouples were amplified, demodulated, and transmitted to a recording multichannel oscillograph. The excitation was furnished by a commercial amplifier (ref. 9) with a frequency response of 300 cycles per second. Excitation for the pressure transducers was furnished by a 20-kc carrier amplifier. This signal was amplified, demodulated, and also transmitted to the recording oscillograph. All test analog signals to the oscillograph were recorded at paper speeds of 100 inches per second. The galvanometers used in the oscillograph were the magnetic type.

A typical oscillograph record of a test run is shown in figure 5. The heating rate values for each thermocouple station were calculated with the aid of its trace record and the following equation:

$$q = c_p \rho L \frac{dT}{dt} \tag{1}$$

This equation is based on the assumption that the wall has negligible resistance to heat flow through the thickness of the material; which is reasonable since the wall material has high thermal diffusivity. Also, the radiation loss is assumed to be zero. This assumption is valid since for black body radiation a loss of only 3 Btu/ft^2 sec requires a wall temperature of 1,600° F, whereas test results indicated that the body temperatures reached in the present program did not exceed 1,000° F during any test run. The value of ρ for silicon bronze is 532 lb/ft^3. The values of c_p as a function of temperature are shown in figure 6. The value of L was the measured wall thickness at each thermocouple location.

Since radiation and conduction along the thin skin were negligible, the aerodynamic heating rates were directly proportional to the slopes of the temperature curves. The heating rate data were reduced by a Fortran program written for the IBM 704 electronic computing machine. The values of dT/dt were determined by a subroutine which found the fifth degree polynomial that gave the best fit, in the least-squares sense, to each oscillograph trace record. The equation was then differentiated at particular times of interest.

The procedure outlined above yields a value of q corresponding to a value of time for each trace record. The heating rates generally decrease with time as a result of the timewise decay of reservoir conditions in the shock tube. Analysis based on the test results of several plain hemisphere models of 1.5-inch diameter indicated that the variation in the stagnation heating rate with test time could be approximated to within ±6 percent of the experimental value by the exponential relationship:

$$q_s(t) = [q_s(t = 0)]e^{-4t} \tag{2}$$

Equation (2) was used to extrapolate the test data to the start of flow ($t = 0$). The time, $t = 0$, is considered to be the time when flow is established over a model, and the data extrapolated to that time represent values that would have been measured but for the response times inherent in the read-out equipment and model. In addition to the timewise decay effects, operating experience has shown that the magnitude of the shock tube pressure (reservoir pressure for the tunnel) varied slightly from run to run. The calculated stagnation-point heat transfer

could be related to the shock-tube pressure by the following empirical relationship;

$$[q_s(t = 0)]_{cal} = -91 + 0.0811 \left(\begin{matrix} \text{shock-tube} \\ \text{pressure,} \\ \text{psi} \end{matrix} \right) \qquad (3)$$

Equations (3) and (2) were used to predict the stagnation-point heat transfer of the models equipped for film cooling. (These models did not have thermocouples located in the stagnation region.)

To standardize the heat-transfer results for both the plain and film-cooled models, the stagnation heating rates used in the data reduction were those calculated by equation (3). To eliminate the decay effects as a variable, the values of $q(t)$ were divided by the stagnation heating rate $[q_s(t)]_{cal}$.

RESULTS AND DISCUSSION

The data were obtained from tests of two types. First, plain models were tested to obtain the heat-transfer rates to the basic hemispherical shape. Second, models equipped for helium ejection in the stagnation region were tested to determine the reduction in heat-transfer rate with film cooling.

Plain Model

The temperature transients at the inner surface of the model were measured by 12 thermocouples distributed along the model as indicated in figure 5. Typical oscillograph records of the temperature rise are also shown on this figure. The starting time of the calculations, as indicated on figure 5, was selected on the basis of the known response time of the instrumentation (about 1.5 milliseconds) and the computed time for the temperature rise rate of the inner surface to reach that of the outer surface (about 15 milliseconds). These latter computations were performed with the method given in reference 10. Figure 7 shows a typical time history of the experimental heat-transfer rates at the stagnation point obtained from the type of record illustrated in figure 5. In figure 7, a comparison is also made of the measured stagnation heating rate for $t = 0$ with that calculated by the method of reference 11.

The variation of the ratio of local to stagnation-point heat-transfer rate as a function of test time is given in figure 8. Although some variation is noted, to within the experimental accuracy this ratio is constant for the test period.

Figure 9 shows the ratio of local to stagnation-point heat-transfer rate as a function of body angle on two hemispherical models. To obtain a smooth curve of the test results, a curve fit was selected with a $\cos^2(A\theta)$ variation where the constant A was determined so that the curve passed through $q(t)/[q_s(t)]_{cal}$ of 0.11 at a body station of 80° (i.e., A = 0.883). For comparison, Lee's theory (ref. 12) is also shown on the figure.

Model With Film Cooling

The tests of film cooling to a hemispherical model in a high-enthalpy stream were exploratory in nature with the primary object of gaining both an understanding of the mechanics of the flow and ascertaining the cooling potentialities of the system with helium as the coolant. Both references 1 and 2 emphasized the necessity of having a matched interface between the coolant gas and the hot gas. Intuitively it could be reasoned that a matched interface is necessary in the stagnation region to preserve the integrity of the helium film as an insulating layer along the body surface. Mixing across the interface would reduce the extent of the region being cooled by substantially increasing the molecular weight of the film gas (helium mixed with air) and by reducing its heat capacity. Reference 2 clearly shows the adverse effects of these changes.

The analysis of reference 2 was based explicitly on the condition that the ratio of velocities of the air and film at their interface was unity. No insight was given as to the effects, if any, of small or large deviations from the value of unity. One of the first problems, then, of the experimental program was to determine the sensitivity of cooling effectiveness to matching the interface velocity.

Typical heat-transfer results for a film-cooled model are presented in figure 10 to show that the values of $q(t)/[q_s(t)]_{cal}$ for a given body station were essentially constant over the test period (to within the accuracy obtained with plain models; see fig. 8).

The distributions of the local heat-transfer rates as a function of body angle for two film-cooled models with different cap arrangements are shown in figure 11. Calculations indicated that with the cap exit located at a body angle of 5°, the ratio of film velocity to the local body velocity, V_f/V_a, was 5.0. With the cap exit at 10°, the value of V_f/V_a was 1.7. For purposes of comparison, the distribution for a plain model is also shown on the figure. It can be noted that the helium flow reduced the heating rates from those of the plain model, particularly in the cap-exit region.

The two local heat-transfer distributions for approximately equal weight rates of helium flow indicate that cooling is dependent on

matching interface velocity. It is not possible, however, to determine the relative importance of interface velocity ratios and of cap-exit locations since both were changed.

The effect of weight rate of helium flow on the distribution of local heating rates, for the closely matched interface velocity as represented by the cap exit at 10° body angle, is shown on figure 12. It can be noted that even at the lowest rate of injection ($w_f = 2.4 \times 10^{-4}$ lb/sec), the heat-transfer rate was appreciably decreased downstream of the cap-exit station. As the injection rate increased, cooling progressively increased. From the figure it can be seen that for the maximum coolant flow rate tested, the peak heating rate was reduced by a factor of about 2.5 from the plain model.

It is of interest to compare the trend and magnitude of the experimental results with those calculated with the intermediate film analysis in reference 2 for the same model geometry and environment. The calculated heating rate distributions are given in figure 13. Particular comparisons of the data from these figures have been arranged in figure 14 to illustrate the effect of coolant flow on local heating rates for the different interface conditions as represented by the two cap positions. In figure 14(a) the data are presented for a body station just downstream of the cap exit. In this location, the length of coolant run along the surface is well within the regime in which mixing between the film and stream gases should be small. It can be noted from the experimental data that the matched interface velocity provided better cooling effectiveness at a given rate of coolant flow. One of the assumptions used in the analysis of reference 2 based on the intermediate-film model concept was that the film replaces just the boundary-layer thickness of air flow. It is estimated that the weight rate of air flow in the laminar hemisphere boundary layer was between 2 and 4×10^{-4} lb/sec (for this particular model and test condition). A comparison of the experimental curves in figure 14(a) with the analytical curve, for weight flow rates greater than about 4×10^{-4} lb/sec, indicates reasonable agreement in both value and trend for V_f/V_a near unity. For V_f/V_a of about 5, the heating rates vary appreciably from the analytical curve. (The value of weight flow rate of 4×10^{-4} lb/sec is less than 1 percent of the rate at which free-stream air is swept out by an area equal to the model base area.)

Figure 14(b) shows the change in the peak heating rates with coolant flow. Although the effects of matching interface velocity at the cap exit can still be noted, the cooling effectiveness is always less than that indicated by the intermediate-film analysis. Two phenomena may contribute to this decrease. First, as the film flow progresses around the model, mixing between the film and stream flows may increase. Secondly, the large increase in the body surface area with increasing body angle may tend to have a destabilizing effect on the flow in the film.

CONCLUDING REMARKS

Results have been presented of an exploratory shock-tunnel investigation of the effectiveness of film cooling in reducing the rate of heat transfer to a hemisphere. Helium was used as the coolant.

Analysis of the data indicates that the effectiveness of the film-cooling technique appears to be dependent on the matching of the velocity of the coolant and the velocity of the gas stream at the injection position. At the best conditions obtained in this program, the film provided almost complete insulation from the stream gases immediately downstream of the exit port. Generally the heat-transfer results in this area were in fair agreement with the intermediate-film analysis of NASA Technical Note D-861.

The peak heating rate was reduced and progressively moved downstream from the injection port as the coolant flow rate was increased. With a small rate of coolant flow, equivalent to an amount less than 1 percent of that of the free-stream air swept by the model, the peak heating was reduced by a factor of about 2.5.

Ames Research Center
National Aeronautics and Space Administration
Moffett Field, Calif., July 26, 1962

REFERENCES

1. Ferri, Antonio, and Libby, Paul A.: The Use of Helium for Cooling Nozzles Exposed to High Temperature Gas Streams. WADC TN 55-318, Mar. 1956.

2. Swenson, Byron L.: An Approximate Analysis of Film-Cooling on Blunt Bodies by Gas Injection Near the Stagnation Point. NASA TN D-861, 1961.

3. Stalder, Jackson R., and Inouye, Mamoru: A Method of Reducing Heat Transfer to Blunt Bodies by Air Injection. NACA RM A56B27a, 1956.

4. McMahon, Howard M.: An Experimental Study of the Effect of Mass Injection at the Stagnation Point of a Blunt Body. Guggenheim Aeronautical Laboratory, California Institute of Technology Hypersonic Research Project Memorandum No. 43, May 1, 1958.

5. Warren, C. Hugh E.: An Experimental Investigation of the Effect of Ejecting a Coolant Gas at the Nose of a Bluff Body. Jour. Fluid Mech., vol. 8, pt. 3, July 1960, pp. 400-417.

6. Libby, Paul A., and Cresci, Robert J.: Experimental Investigation of the Downstream Influence of Stagnation Point Mass Transfer. Jour. Aero/Space Sci., Jan. 1961.

7. Cunningham, Bernard E., and Kraus, Samuel: A 1-Foot Hypervelocity Shock Tunnel in Which High-Enthalpy, Real-Gas Air Flows Can be Generated With Flow Times in Excess of 180 Milliseconds. NASA TN D-1428, 1962.

8. Clarke, A. E., Jr.: Castings With Ultrathin Walls. Product Engineering, vol. 32, no. 9, Feb. 27, 1961, pp. 42-44.

9. Anon.: The Fitgo Amplifier. Bulletin 3015-c, Beckman Systems, Anaheim, Calif., 1960.

10. Cresci, Robert J., and Libby, Paul A.: Some Heat Conduction Solutions Involved in Transient Heat Transfer Measurements. WADC TN 57-236, Sept. 1957.

11. Fay, J. A., and Riddell, F. R.: Theory of Stagnation Point Heat Transfer in Dissociated Air. Jour. Aero. Sci., vol. 25, no. 2, Feb. 1958, pp. 73-85, 121.

12. Lees, Lester: Laminar Heat Transfer Over Blunt-Nosed Bodies at Hypersonic Flight Speeds. Jet Propulsion, vol. 26, no. 4, April 1956, pp. 259-269, 274.

13. Anon.: Test Report on Specific Heat of Silicon Bronze Metal Samples Supplied by NASA. Test Rep. No. 61-1123, Thermatest Laboratories, Inc., Sunnyvale, Calif., June 29, 1961.

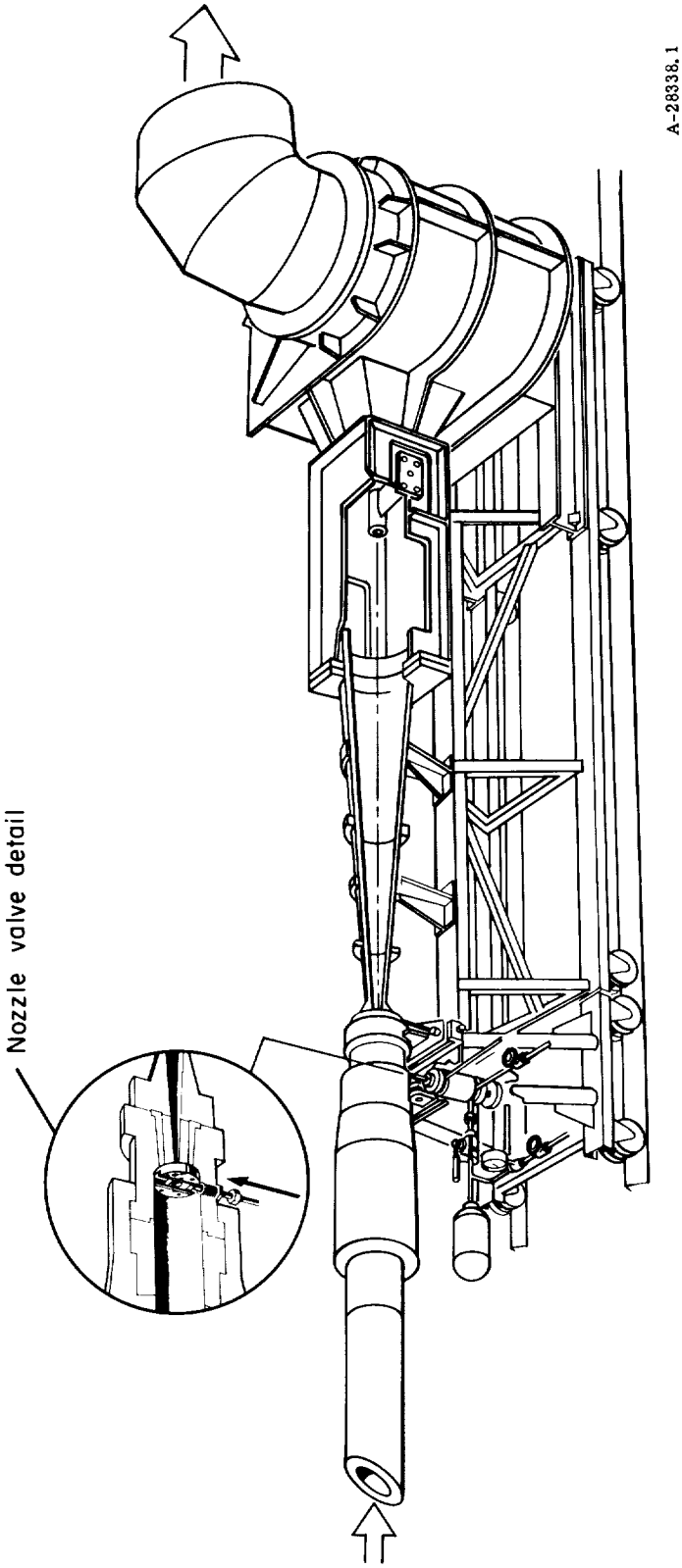

Figure 1.- Schematic drawing of 1-foot hypervelocity shock tunnel.

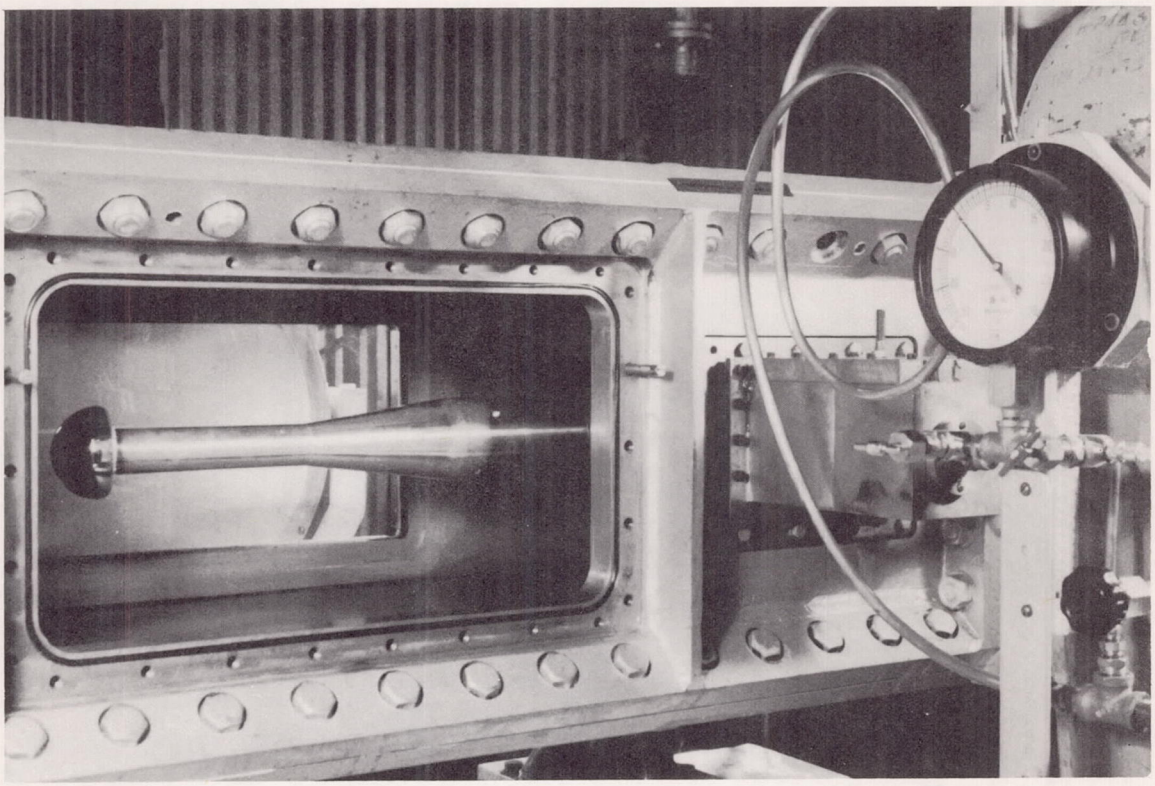

A-26899

Figure 2.- Model installation in test section.

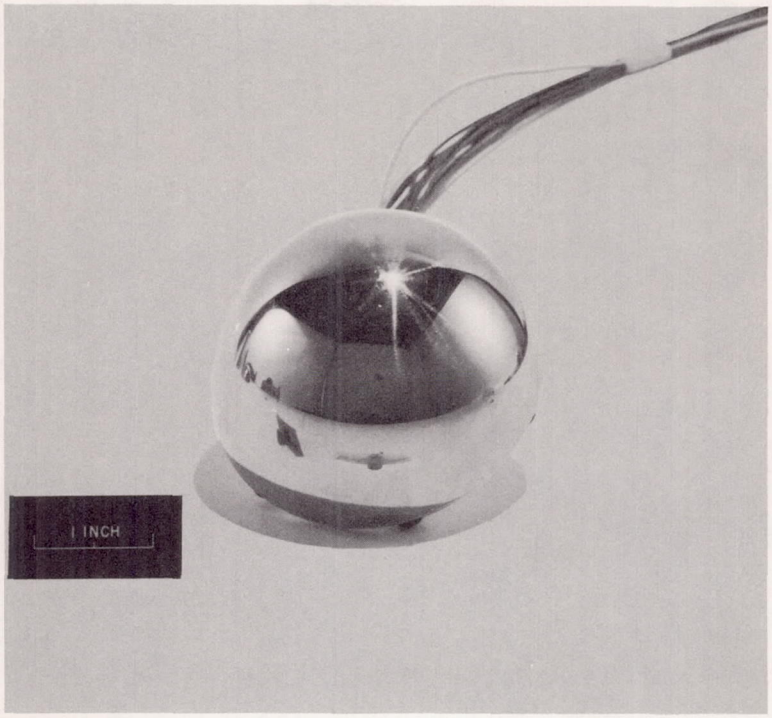

A-26877.1

(a) Plain model.

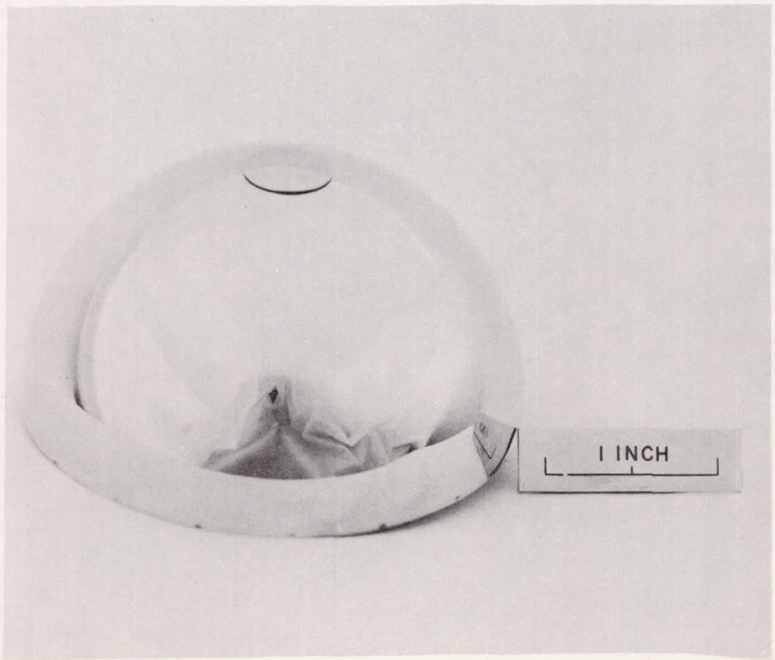

A-27294

(b) Model equipped for film cooling; cap exit at body station of 10°.

Figure 3.- Typical test models.

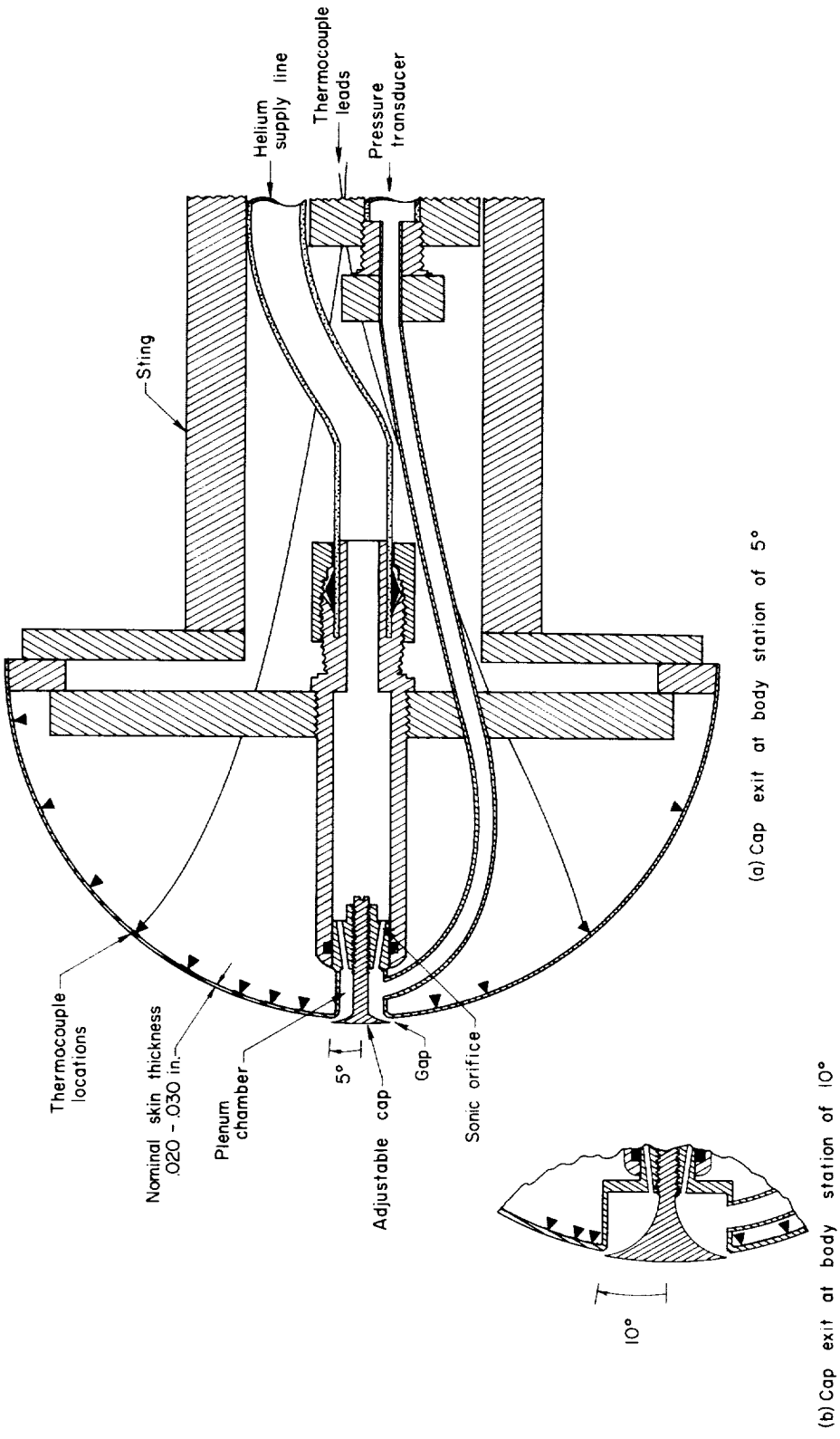

Figure 4.- Sketch of 3-inch-diameter models equipped for film cooling.

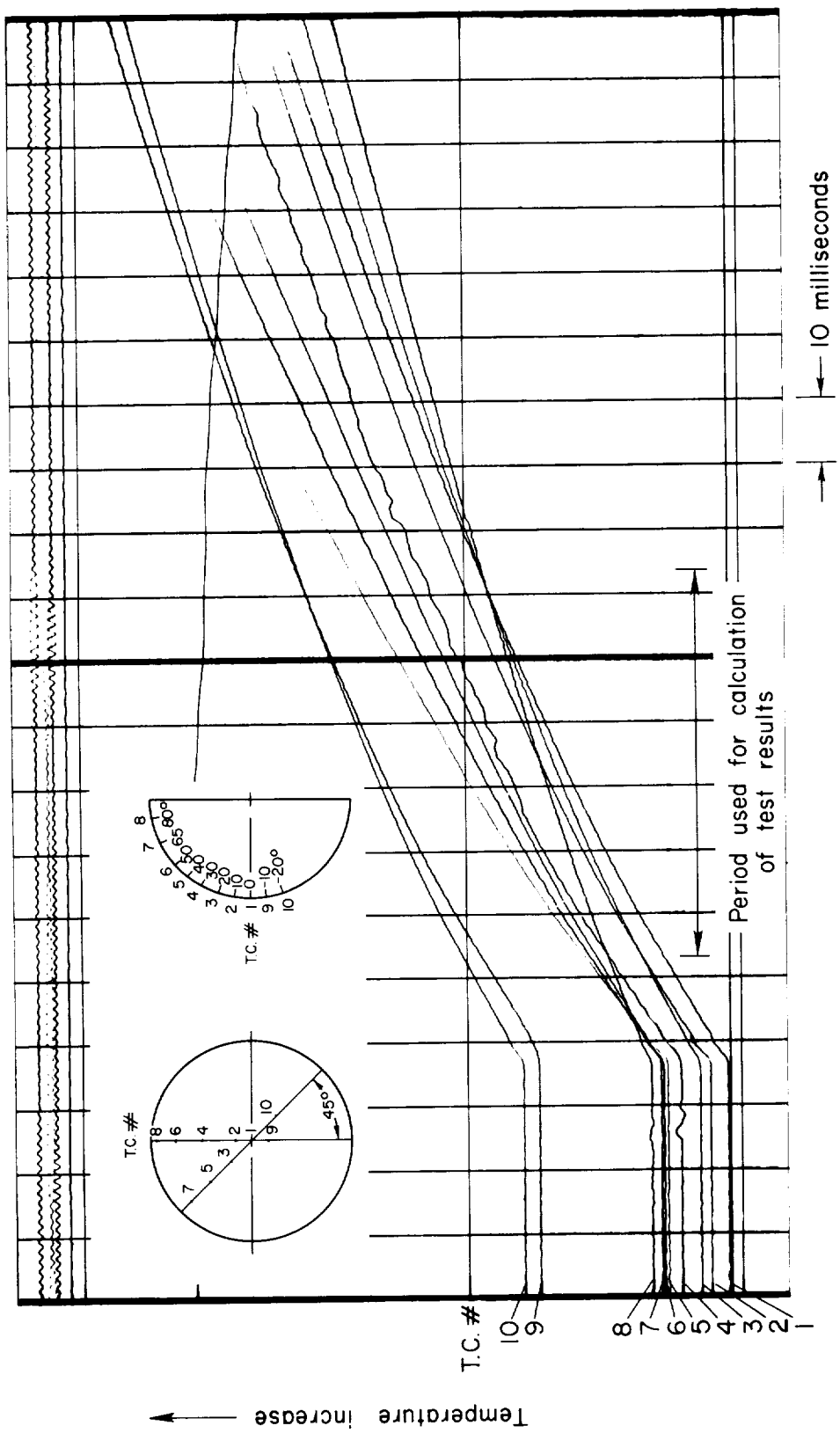

Figure 5.- Typical oscillograph record for a test run of a 3-inch-diameter plain hemisphere model.

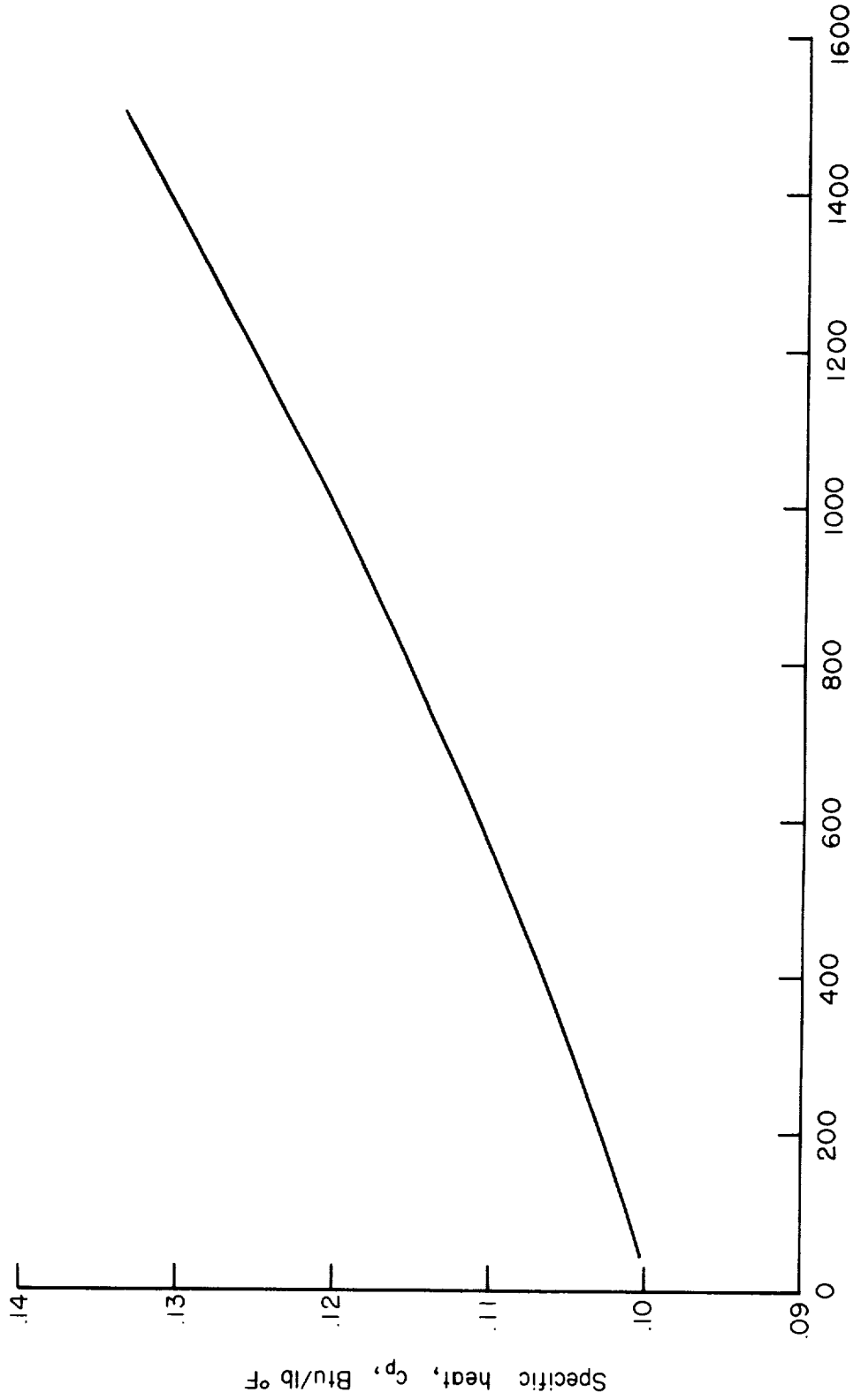

Figure 6.- Specific heat of the silicon bronze metal used in the test program (ref. 13).

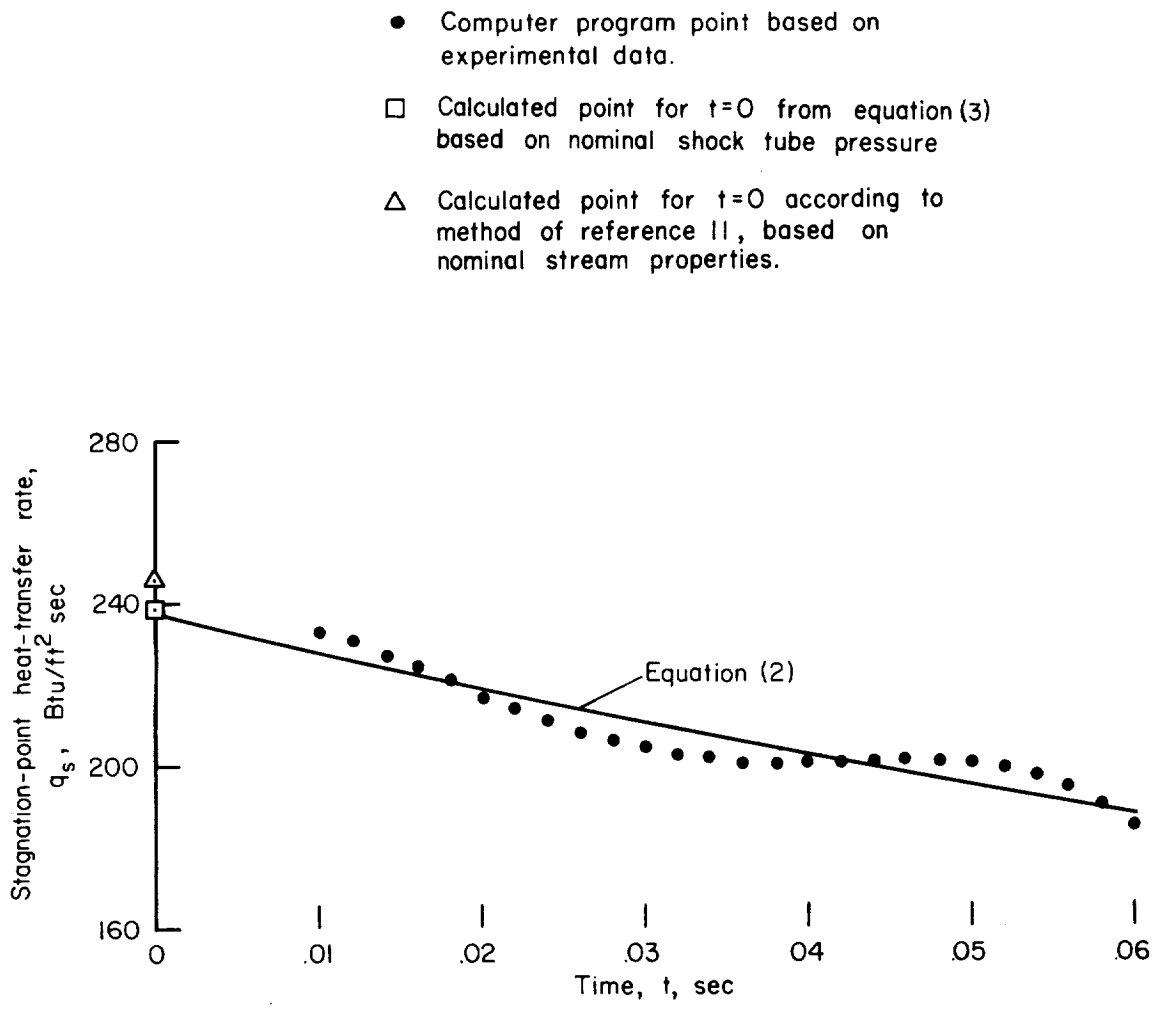

Figure 7.- Correlation of experimental with analytical values from equations (2) and (3) of stagnation-point heat-transfer rate for a plain hemisphere model.

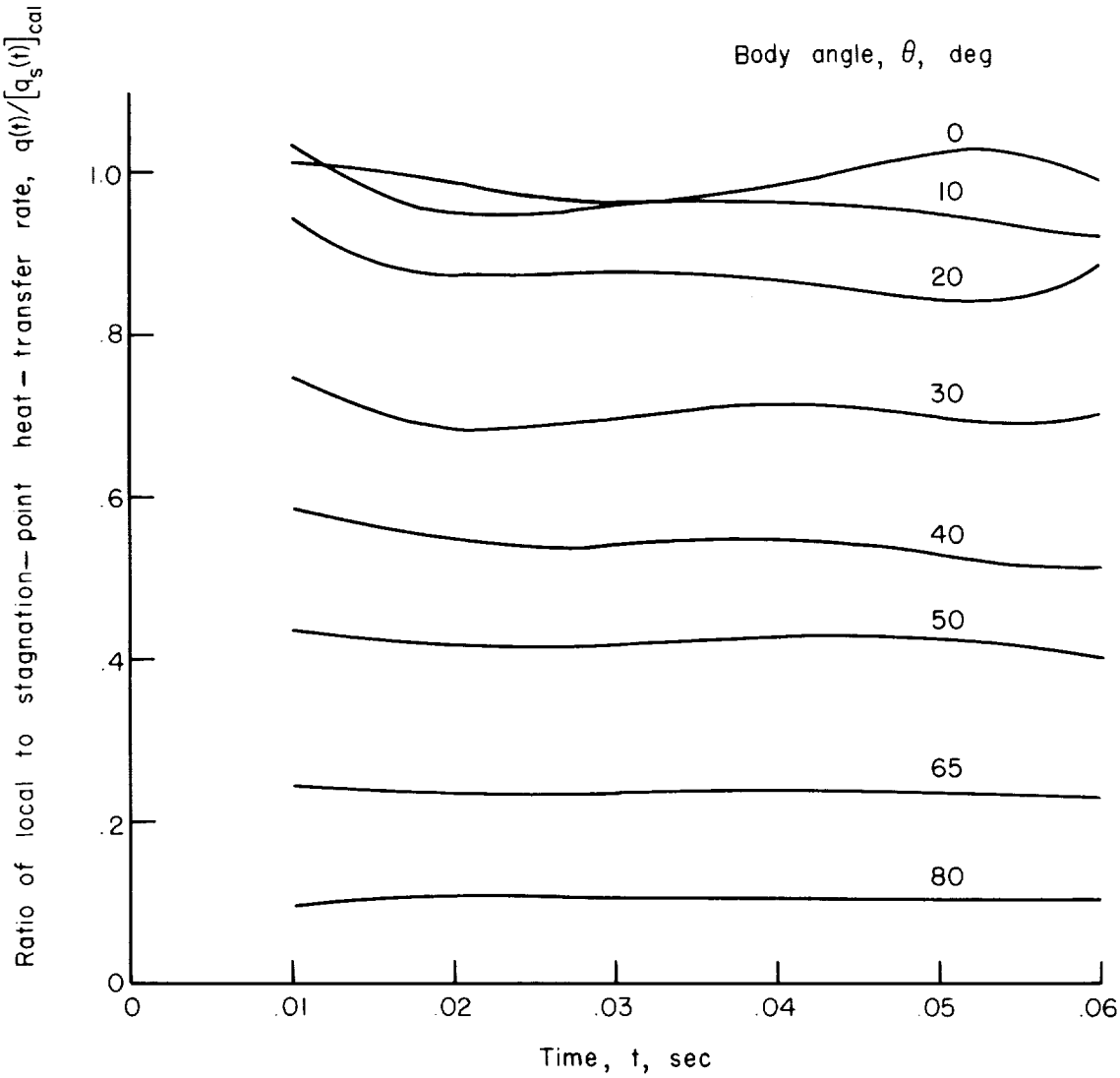

Figure 8.- Variation of local heat transfer with test time on a plain hemisphere model.

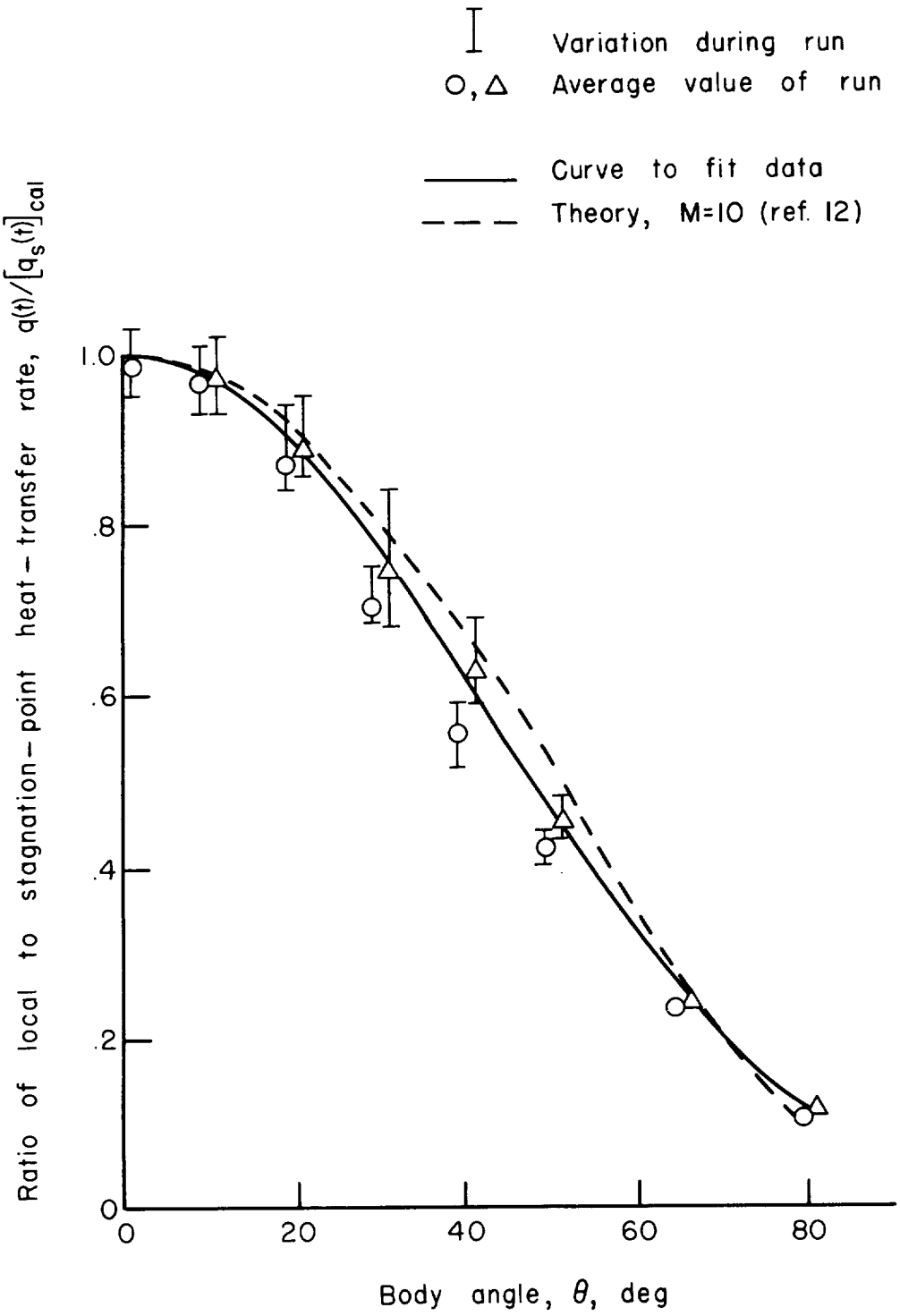

Figure 9.- Distribution of local heat transfer over plain hemisphere models.

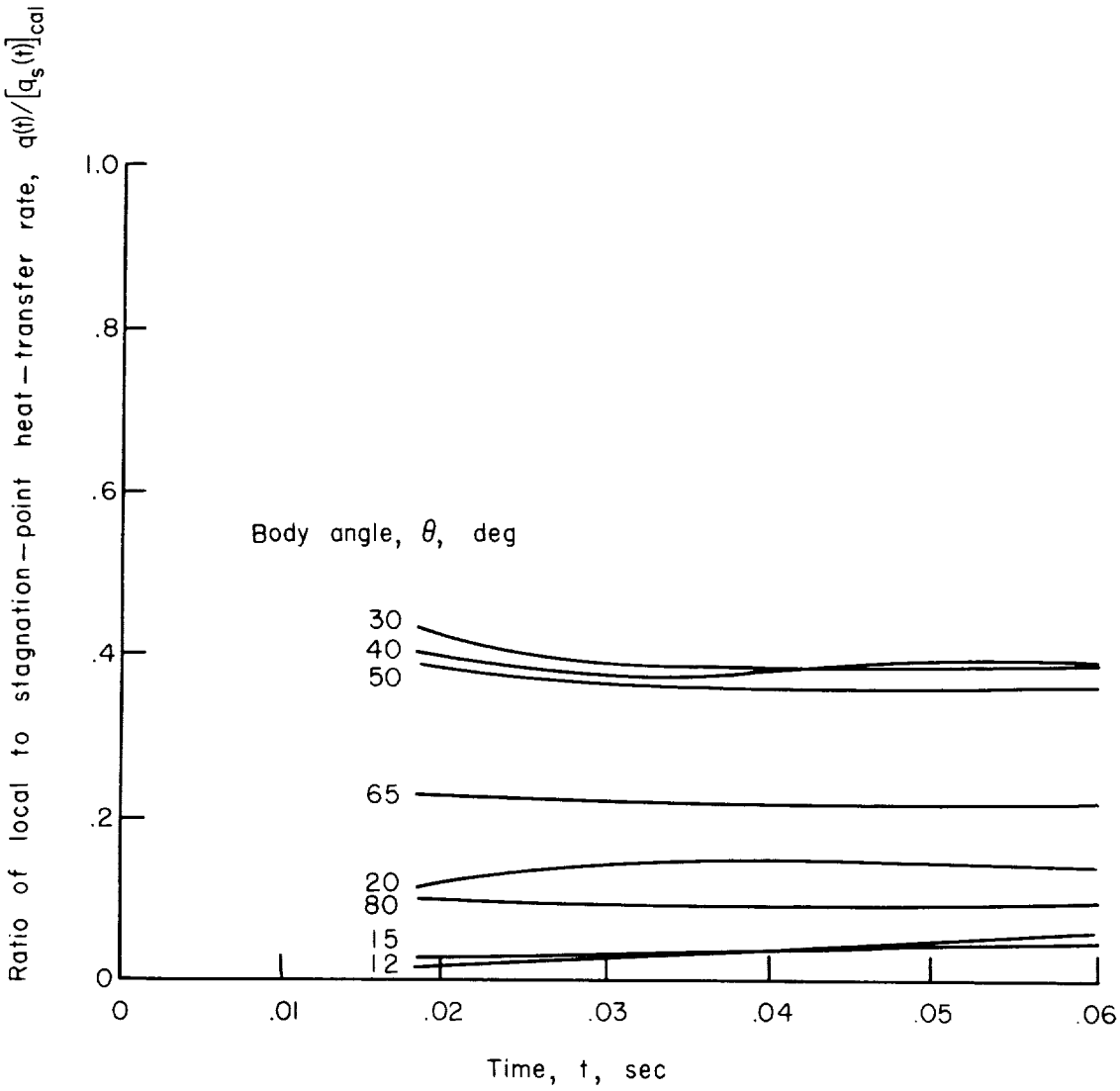

Figure 10.- Variation of local heat transfer with test time on a hemisphere model equipped for helium injection; cap exit at body station of 10°; $w_f = 11.8 \times 10^{-4}$ lb/sec; $V_f/V_a = 1.2$.

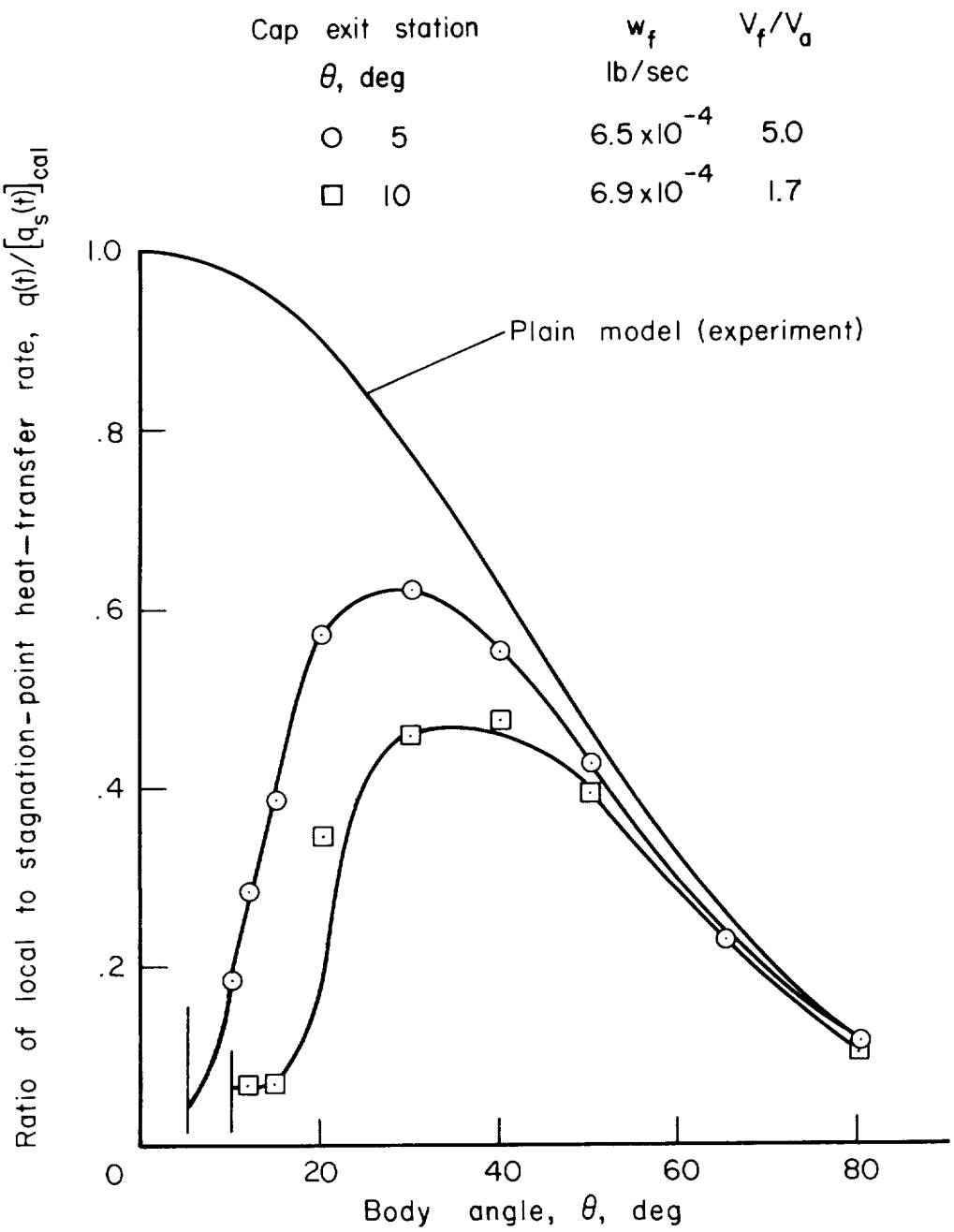

Figure 11.- Comparison of local heat transfer on a hemisphere with helium injection for different air-helium interface velocities at the cap exit.

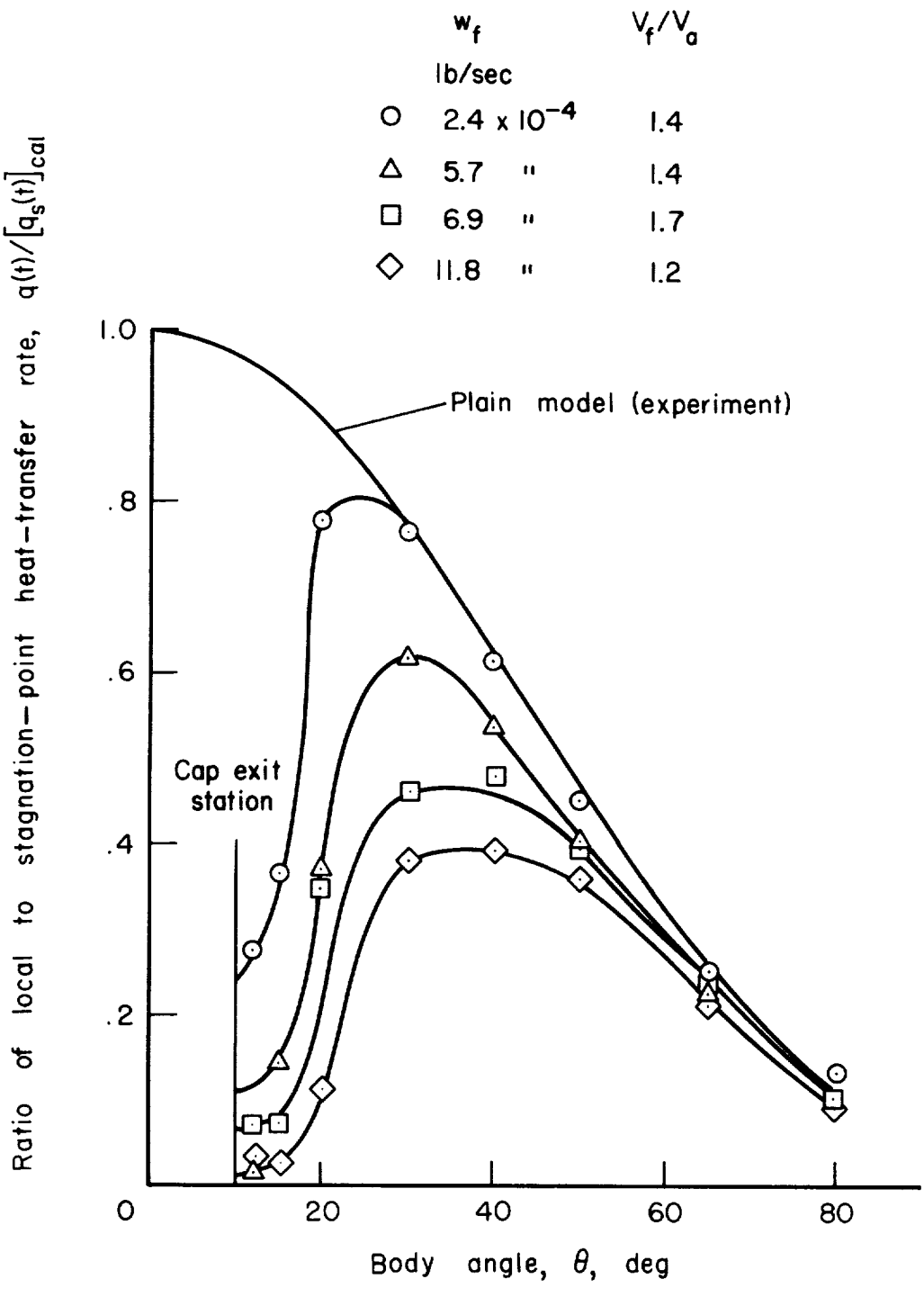

Figure 12.- Comparison of local heat transfer over a hemisphere with helium injection at body station of 10°.

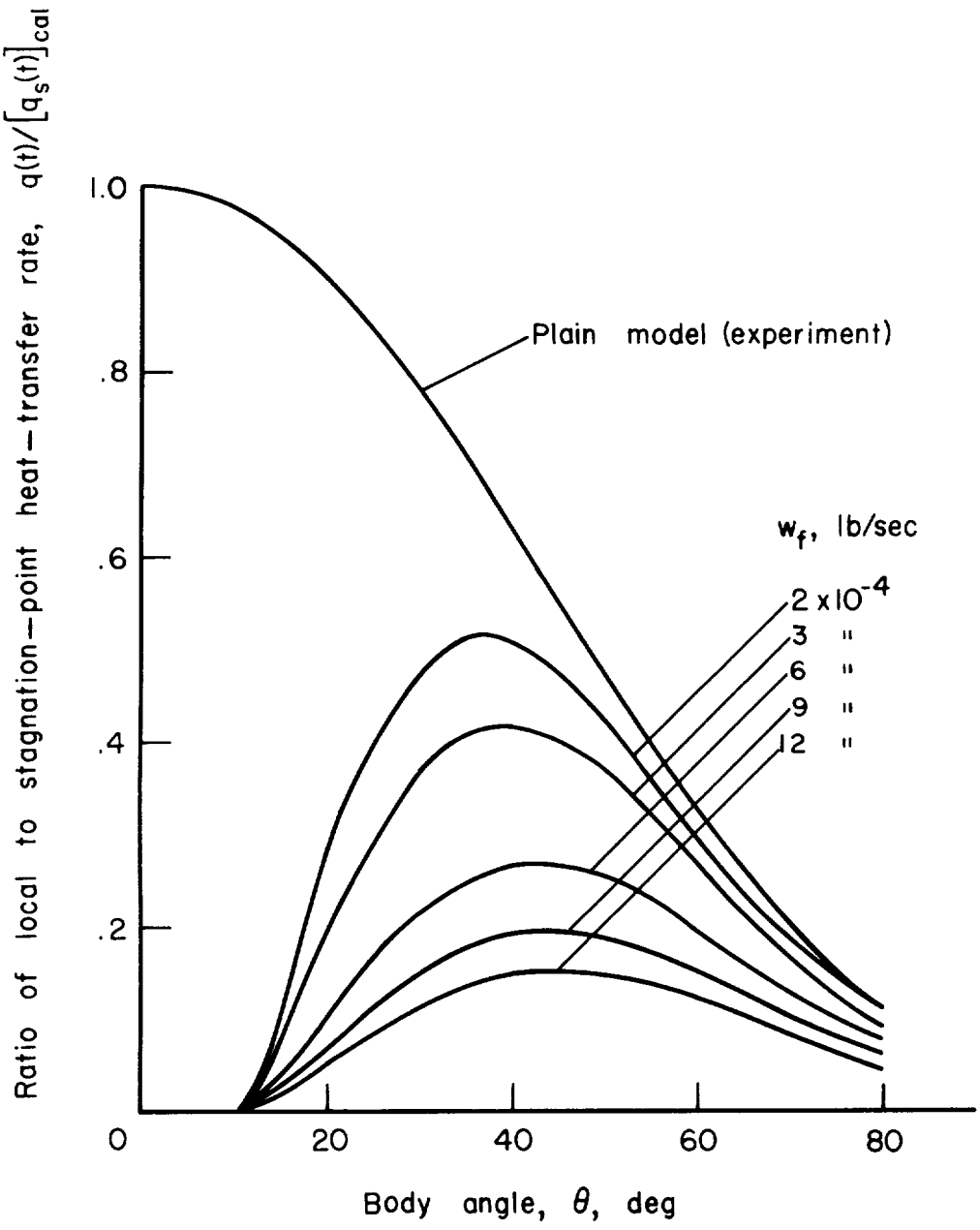

Figure 13.- Comparison of calculated effects of helium film flow on reduction and distribution of local heat transfer to a hemisphere; cap exit at body station of 10°; intermediate film analysis, ref. 2.

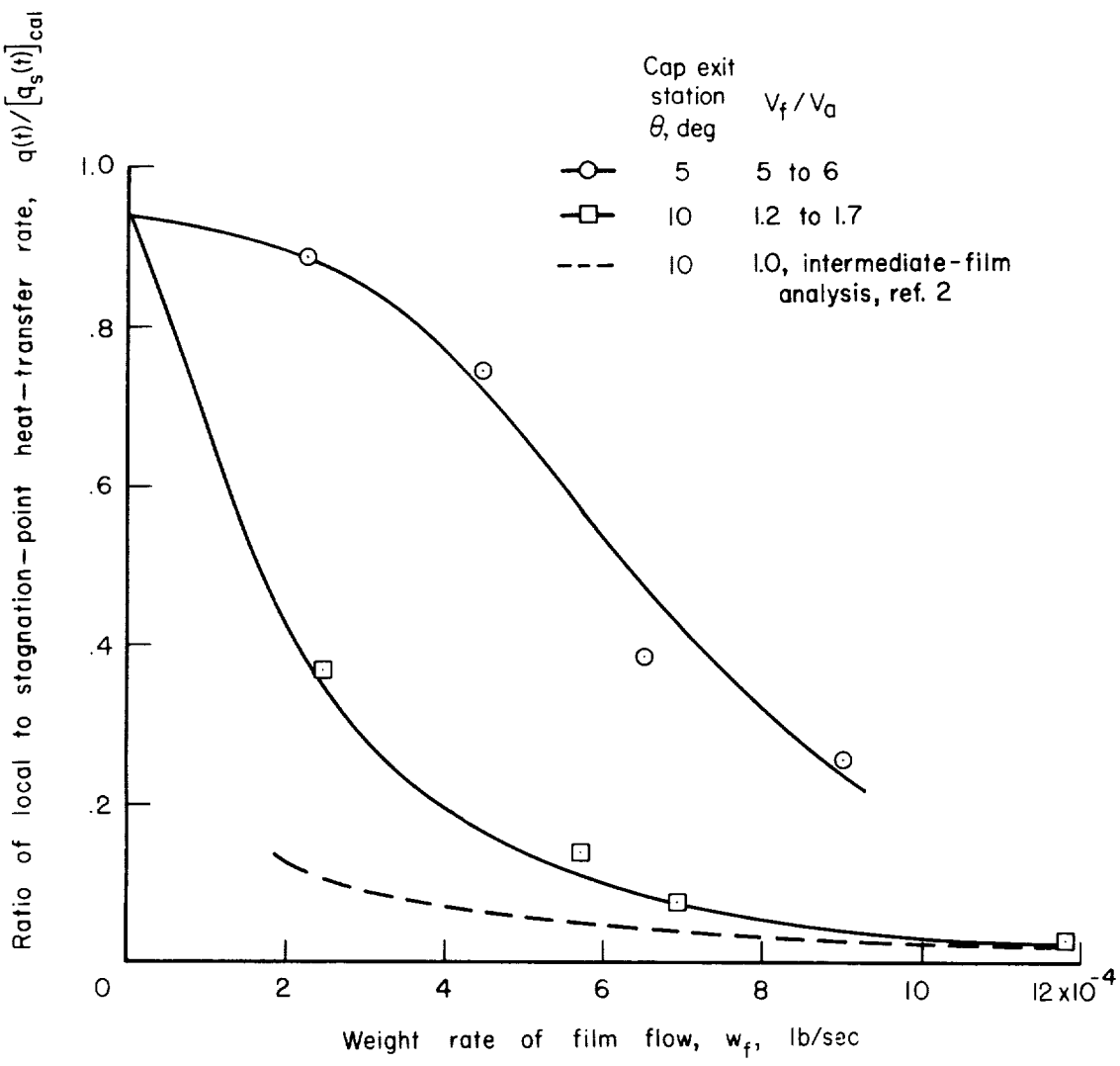

(a) Body station of 15°.

Figure 14.- Comparison of analytical and experimental results of the air-helium interface at the cap exit on the local heat transfer to a hemisphere.

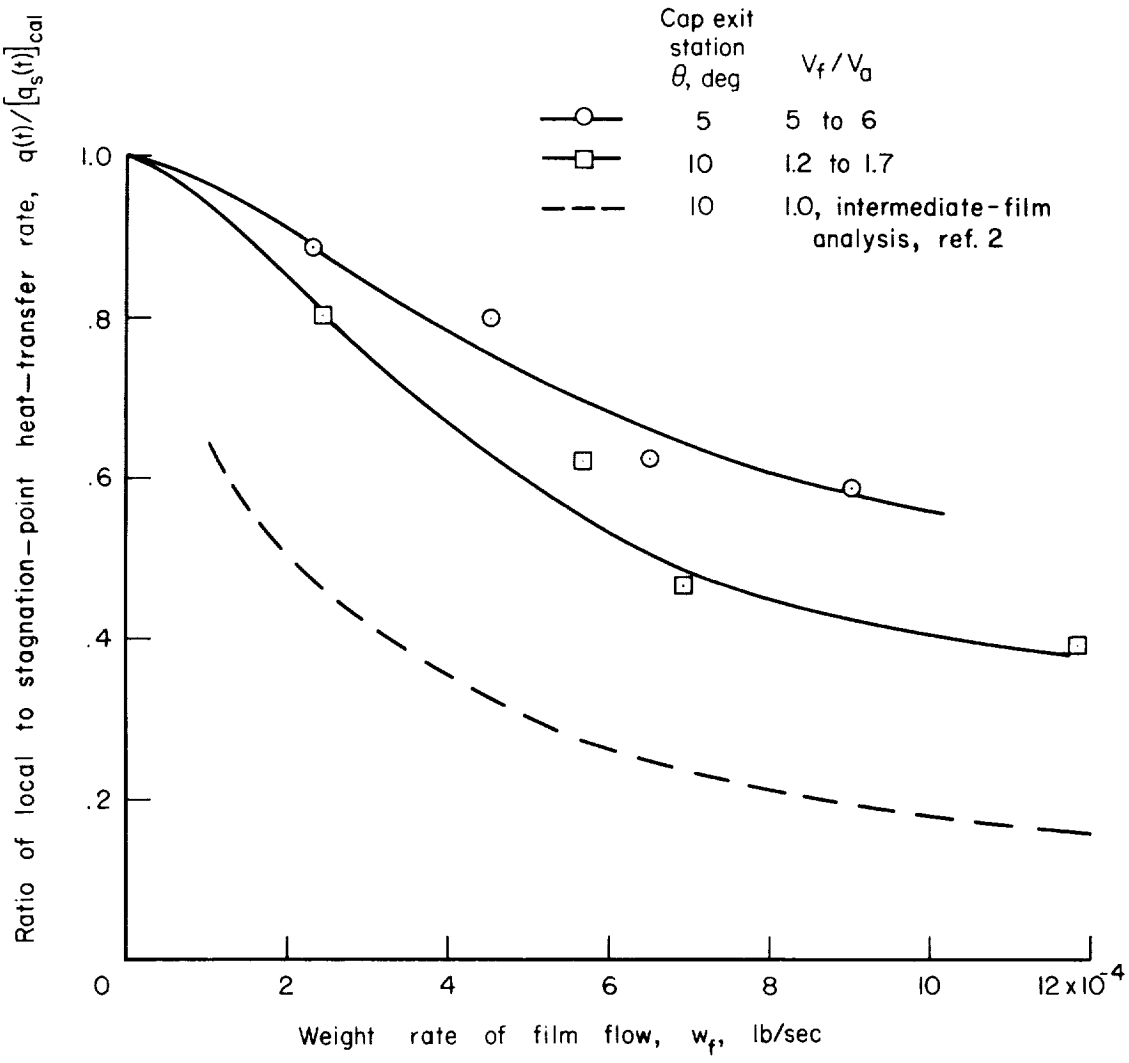

(b) Peak heating.

Figure 14.- Concluded.